DC Link Currents in Frequency Domain for Three-Phase AC/DC/AC PWM Converters

Young-Wook Park Dong-Choon Lee Jul-Ki Seok
School of Electrical Engineering and Computer Science, Yeungnam University
214-1, Daedong, Kyongsan, Kyongbuk, 712-749, KOREA
Tel : 82-53-810-1529, Fax : 82-53-813-8230, dclee@yu.ac.kr

Abstract – **In this paper, dc link ripple currents for three-phase ac/dc/ac PWM converters are analysed in a frequency domain. The expression of the harmonic currents is developed by using switching functions and exponential Fourier series expansion. The dc link ripple currents with regard to power factor and modulation index are investigated. In addition, the effect of the displacement angle between the switching periods of line-side converters and load-side inverters on the dc link ripple current is studied. The result of the dc link current analysis is helpful in specifying the dc link capacitor size and its lifetime estimation.**

I. INTRODUCTION

In recent, the three-phase ac/dc/ac PWM converters are increasingly used for industrial applications such as mill drives, elevators, UPS, and so on. The ac/dc/ac PWM converters usually have a dc link with large electrolytic capacitors. The capacitor filter size and its lifetime are dependent on the rms value of the dc ripple currents, more strictly speaking, on each harmonic component.[1] So, it is necessary to analyze the frequency spectrum of the dc link ripple currents.

There are some research results to analyze the dc link ripple currents[2,3], where only the rms value of the ripple currents was developed. The published papers, which dealt with the frequency spectrum of the dc link current, are very a few[4,5]. In [4], the dc link current in PWM inverters only was analyzed and in [5] the frequency spectrum was presented experimentally not analytically.

In this paper, dc link ripple currents for three-phase ac/dc/ac PWM converters are analyzed in a frequency domain. The expression of the harmonic currents is developed by using switching functions and exponential Fourier series expansion. The dc link ripple currents with regard to modulation index and power factor are investigated. In addition, the effect of the displacement angle between the switching periods of line-side converter and load-side inverter on the dc link ripple currents is studied. The validity of analysis results has been verified by simulation results.

II. PROCEDURE OF ANALYSIS

Fig.1 shows the main circuit of three-phase ac/dc/ac PWM converter. The procedure to derive the dc link ripple current, which basically comes from [4] where analysis of the inverter input current only has been developed, is as follows;

i) Each phase current of the inverter, i_k, is calculated from n-th harmonic voltages.

ii) Dc link current due to a phase is determined by multiplying the phase current by the switching function applied to that phase.

$$i_{dck} = i_k \cdot S_k \tag{1}$$

iii) The sum of the contribution of the three phases gives the total dc link current drawn by the inverter such as

$$i_{dcI} = \sum_{k=1}^{3} i_k \cdot S_k \tag{2}$$

iv) In the same way as above except additively considering the source voltage, $e_{a,b,c}$, the dc link current of the converter output terminal, i_{dcR}, is calculated.

$$i_{dcR} = \sum_{k=1}^{3} i_k \cdot S_k \tag{3}$$

v) The ripple current of the dc link capacitor is calculated by adding vectorially both the harmonics of the converter output and the inverter input terminals, considering a displacement angle, which is expressed as

$$\overset{\rho}{i}_{Cn} = \overset{\rho}{i}_{dcRn} + \overset{\rho}{i}_{dcIn} \cdot e^{j\varphi_{st}} \tag{4}$$

where, φ_{st} is an angle displaced between the two switching periods of the converter and the inverter. This angle plays a role of a control parameter, which can reduce the dc link ripple current. The vector summation of both the currents should be referred to the angles of the PWM voltage reference of the converter and the inverter, which are in phase.

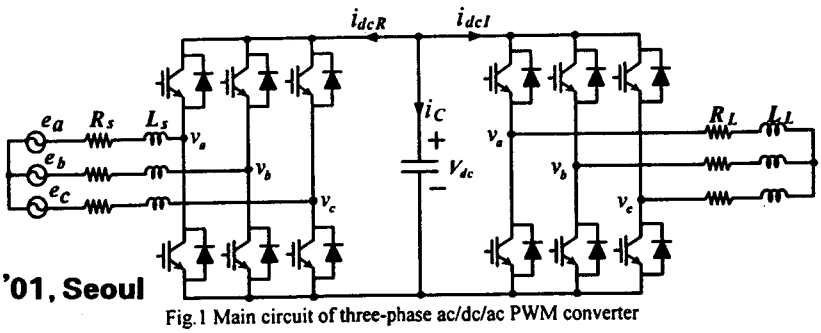

Fig.1 Main circuit of three-phase ac/dc/ac PWM converter

III. EXPRESSION OF SWITCHING PULSES

Fig. 2(a) shows switching pulses by triangular comparison, from which switching function and pole voltage waveform are determined. Fig. 2(b) shows one of switching pulses.

The fundamental period is subdivided into p short pulses with equal width Δ.

$$\Delta = 2\pi / p \tag{5}$$

The angle of δ_{1i} and δ_{2i} means a certain pulse width in a switching period. δ_0 is the quarter of a pulse width. If $\delta_{1i} = \delta_{2i} = \delta_0$, then the average voltage over the pulse is zero.

Considering the left-half pulse, the average voltage over this period V_{1i} is

$$V_{1i} = \beta_{1i}(0.5V_{dc}) \tag{6}$$

$$\text{where, } \beta_{1i} = \frac{\delta_{1i} - \delta_0}{\delta_0} \tag{7}$$

In high switching frequency PWM, the average voltage during half a period of PWM pulse is proportional to the amplitude of the sine wave V_m. So,

$$\beta_{1i}(0.5V_{dc}) \propto V_m \sin(\alpha_i - \delta_o) \tag{8}$$

where, V_{dc} is the dc link voltage.

When the amplitude of the sine wave is expressed with modulation index M,

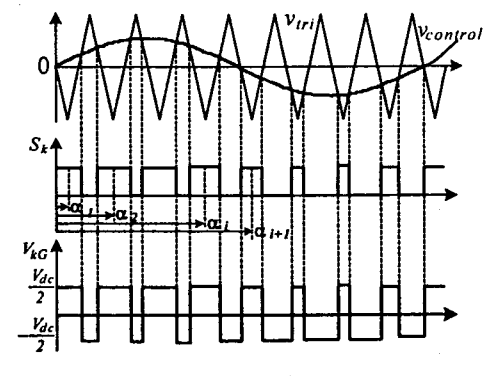

(a)

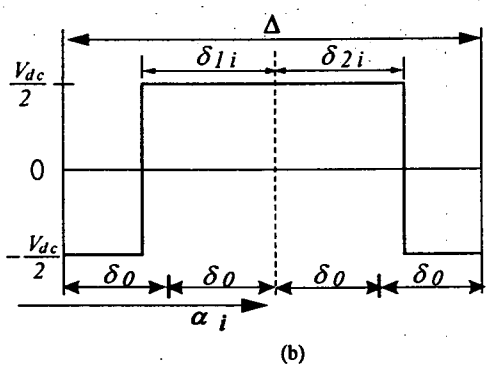

(b)

Fig. 2. Sinusoidal pulse width modulation and a cycle of PWM waveform

$$V_m = M(0.5V_{dc}) \tag{9}$$

Then,

$$\beta_{1i} = M\sin(\alpha_i - \delta_o) \tag{10-a}$$

Similarly,

$$\beta_{2i} = M\sin(\alpha_i - \delta_o) \tag{10-b}$$

By substituting for β using (7), (10) are expressed in an alternative form as

$$\delta_{1i} = \delta_o[1 + M\sin(\alpha_i - \delta_o)] \tag{11-a}$$

$$\delta_{2i} = \delta_o[1 + M\sin(\alpha_i + \delta_o)] \tag{11-b}$$

Eqs. (11) define the modulating law for the PWM strategy.

The amplitude of the n-th harmonic components due to the i-th pulse C_{ni} is given by

$$C_{ni} = j(\frac{1}{2\pi n})\{e^{-jn\delta_{2i}} - e^{jn\delta_{1i}}\}e^{-jn\alpha_i} \tag{12}$$

where, j means an imaginary unit in complex number.

For the p pulses in a fundamental period,

$$C_n = \sum_{i=1}^{p} C_{ni} \tag{13}$$

The harmonic coefficients of the switching function S_k and the modulated pole voltage are the same since the latter are obtained from the former, which is multiplied by V_{dc} and subtracted by the average value.

IV. ANALYSIS OF DC LINK CURRENTS

Using the harmonic coefficient of the switching function and the pole voltage, the dc link current of the both-side converters can be found.

A. Derivation of phase currents of inverter

The three-phase inverter circuit is shown in Fig. 3. If the amplitude of the n-th harmonic component of the pole voltage of the k-th leg is denoted by V_{kGn}, the corresponding harmonic currents i_{kn} is given by

$$i_{kn} = \frac{V_{kGn}}{Z_{kn}} \tag{14}$$

where, Z_{kn} is the impedance to the n-th harmonic

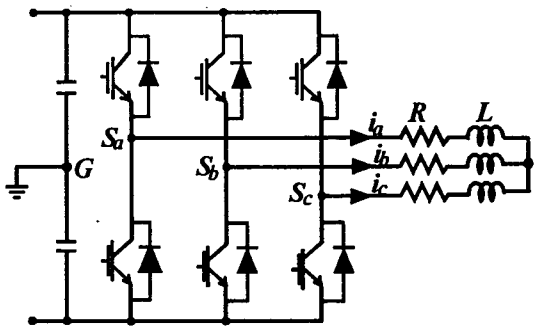

Fig. 3. Three-phase PWM inverter

frequency between terminals of each leg and virtual dc link middle point. The leg current is given by

$$i_k = \sum_{n=-\infty}^{n=\infty} (\frac{V_{kGn}}{Z_{kn}}) e^{jn(\theta-\phi)} \cdot e^{-jn2\pi(k-1)/3} \quad (15)$$

where, ϕ is impedance angle of the load.

The last term in (15) means that k-th leg current is displaced by $2\pi/3$ compared with $(k+1)$-th leg current. The sum of all the three leg currents is given by

$$i_o = \sum_{k=1}^{3} i_k \quad (16)$$

$$= \sum_{k=1}^{3} \{ \sum_{n=-\infty}^{\infty} (\frac{V_{kGn}}{Z_{kn}}) e^{jn(\theta-\phi)} \cdot e^{-jn2\pi(k-1)/3} \} \quad (17)$$

If the impedances in all legs are the same, i.e. $Z_{kn} = Z_n$, (17) can be rearranged as

$$i_o = \sum_{n=-\infty}^{\infty} \{ (\frac{V_{kGn}}{Z_n}) e^{jn(\theta-\phi)} \sum_{k=1}^{3} e^{-jn2\pi(k-1)/3} \} \quad (18)$$

In (18), by a geometric series,

$$\sum_{k=1}^{3} e^{-jn2\pi(k-1)/3} = e^{-jn2/3} \frac{\sin(n\pi)}{\sin(n\pi/3)} \quad (19)$$

The sine term in (19) is zero for any integer n except that $n \neq 3 \cdot s,\ s = 0, \pm 1, \pm 2, \Lambda$.

Since triplen harmonic components cannot exist at the load of the three-phase inverter, (15) is expressed as

$$i_k = \sum_{n=-\infty}^{n=\infty} (\frac{V_{kGn}}{Z_{kn}}) e^{jn(\theta-\phi)} \cdot e^{-jn2\pi(k-1)/3}$$
$$n \neq 3 \cdot s,\ s = 0, \pm 1, \pm 2, \Lambda \quad (20)$$

B. Derivation of switching function S_k

The switching function S_k is expressed as

$$S_k = \sum_{m=-\infty}^{\infty} C_m \cdot e^{jm\theta} \cdot e^{-jm2\pi(k-1)/3} \quad (21)$$

which is similar to (20) with the coefficient of (21).

C. Derivation of total dc link currents of inverter

The total DC link current is given by

$$i_{dcl} = \sum_{k=1}^{3} \{ \sum_{n=-\infty}^{\infty} (\frac{V \cdot C_n}{Z_n}) \cdot e^{jn(\theta-\phi)} \cdot e^{-jn2\pi(k-1)/3}$$
$$\times \sum_{m=-\infty}^{\infty} C_m e^{jm\theta} \cdot e^{-jm2\pi(k-1)/3} \} \quad (22)$$

By geometric series,

$$\sum_{k=1}^{3} e^{-j2\pi(k-1)(m+n)/3} = e^{-j2\pi(m+n)/3} \frac{\sin\pi(m+n)}{\sin\pi(m+n)/3} \quad (23)$$

Substituting (23) into (22), i_{dcl} becomes zero unless $m+n = 3s', (s' = 0, \pm 1, \pm 2, \Lambda)$ where, the sine quotient becomes three. Hence, (23) is simplified to

$$i_{dcl} = \sum_{n=-\infty}^{\infty} \sum_{m=-\infty}^{\infty} 3 \cdot (\frac{V \cdot C_n}{Z_n}) \cdot C_m \cdot e^{js'3\theta} \cdot e^{-jn\phi} \cdot e^{-j2\pi s'} \quad (24)$$

where, $n \neq 3s,\ s = 0, \pm 1, \pm 2, \Lambda$,
$m + n = 3s',\ s' = 0, \pm 1, \pm 2, \Lambda$.

Eq. (24) is the general expression for the inverter side dc link current in the time domain.

On the other hand, the exponential form of the Fourier series of the i_{dcl} is defined as

$$B_l = \frac{1}{2\pi} \cdot \int_0^{2\pi} i_{dcl} \cdot e^{-jl\theta} d\theta \quad (25)$$

where, B_l means the magnitude of the l-th harmonic component of the i_{dcl} . Substituting (24) into (25),

$$B_l = \sum_{n=-\infty}^{\infty} \sum_{m=-\infty}^{\infty} 3 \cdot (\frac{V \cdot C_n}{Z_n}) \cdot C_m \cdot e^{-jn\phi} \cdot e^{-j2\pi s'} \quad (26)$$

where, $n \neq 3s,\ s = 0, \pm 1, \pm 2, \Lambda$,
$m + n = 3s', s' = 0, \pm 1, \pm 2, \Lambda$.

Only for $l = 3s'$, the nonzero harmonics are present.

Eq. (26) is the general expression for the harmonic content of the dc link current in frequency domain. It should be noted that the only harmonic currents present in the dc link of a three-phase inverter are triplen components.

D. Dc link current through capacitors

The dc link current of the line-side converter is derived just as (26) except that the ϕ is replaced by the phase angle difference between the modulated voltage and the current of the converter and that the effect of the source voltage should be considered in calculating i_{kn} of (14) as

$$i_{kn} = \frac{V_{kGn} - Ee^{j(\omega_e t + \phi)}}{Z_{kn}} \quad (27)$$

where, E and ω_e are the magnitude and the angular velocity of the source voltage, respectively.

Finally, frequency spectrum of the dc link ripple current through the capacitor is found by a vector combination of each harmonic component of both the converter and inverter as

$$\underset{i_{Cn}}{\rho} = \underset{i_{dcRn}}{\rho} + \underset{i_{dcIn}}{\rho} \cdot e^{j\varphi_{st}} \quad (28)$$

Fig. 4 shows dc link current waveforms of PWM converter and inverter. The displacement angle corresponds to the distance between the middle points of the interval T_o of both switching cycles.

Minimum of the rms ripple current are obtained at $\varphi_{st} = 0, \pi, 2\pi$. For these values the superposition of the freewheeling states of both converters is maximum. In the case of $\varphi_{st} = \pi/2, 3\pi/2$ the superposition of the freewheeling states is minimum or missing and the rms value is maximum. This angle provides an additional degree of freedom for the PWM control, by the control of which the dc link ripple currents can be minimized.

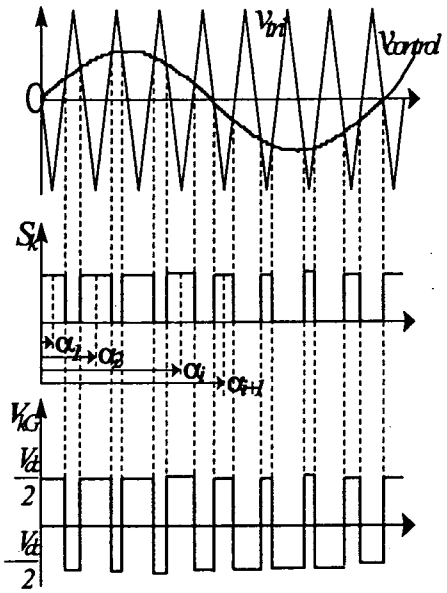

Fig. 4. Switching pulses and displacement angle
top; inverter, bottom; converter

V. ANALYSIS RESULTS AND DISCUSSIONS

The results of the analysis are illustrated by using Mathcad and to verify the validity, PSIM simulation has also been carried out.

The system model is as follow; the source voltage is three-phase $V_s = 220[V]$ and $60[Hz]$. The dc link voltage $V_{dc} = 350[V]$ and the dc link capacitor is $3300[\mu F]$. The operating conditions of the system are listed in Table 1.

Fig. 5 shows dc link current waveforms in time domain. The current envelope at the PWM converter side is continuous, however that of at the PWM inverter side is discontinuous. This discontinuity at the inverter side is due to the lagging current.

Fig. 6 and 7 show the frequency spectrum corresponding to dc link currents in Fig. 5, which resulted from analytic method and PSIM simulation, respectively. Here, the displacement angle was set as zero degree. Both spectra coincide well with each other.

Fig. 8 shows the harmonic spectrum of the inverter input current for asynchronous PWM. The magnitude of each harmonic component is nearly unchanged in spite of asynchronous modulation.

Table 1. Operating conditions.

	Converter side	Inverter side
R, L	1[Ω], 6[mH]	7.52[Ω], 15[mH]
Power factor	1	0.8
Modulation index	1	0.8
Switching/fundamental Frequency	3420/60 [Hz] 57pulses per cycle	3420/60 [Hz] 57pulses per cycle

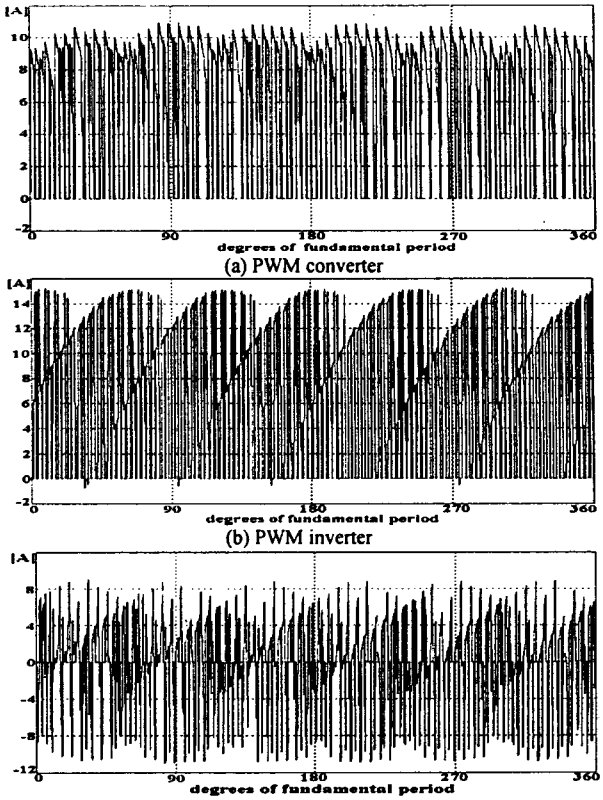

(a) PWM converter

(b) PWM inverter

(c) Dc link capacitor

Fig. 5. Dc link current waveform in time domain

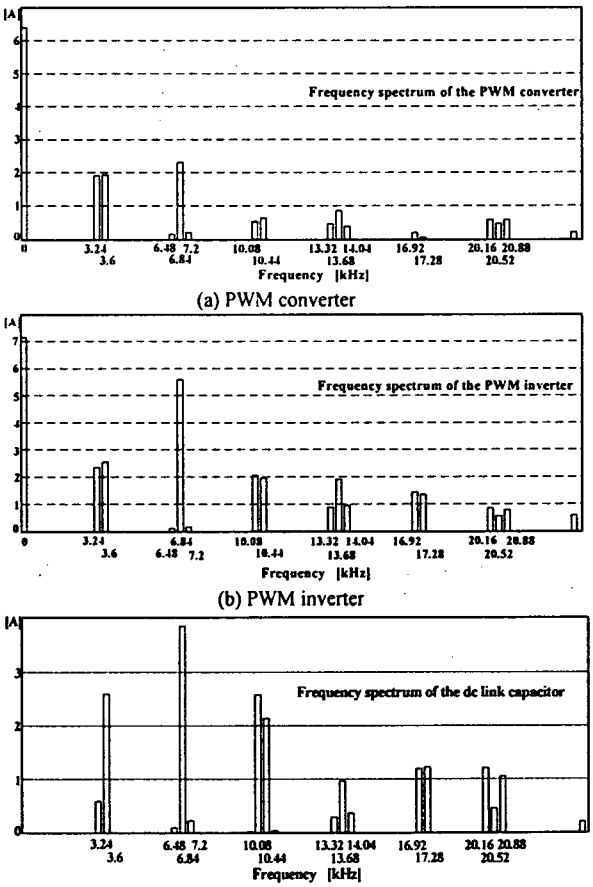

(a) PWM converter

(b) PWM inverter

(c) Dc link capacitor

Fig. 6. Harmonic spectrum of dc link current(analysis)

Fig. 9 shows the rms value of the dc link ripple currents with regard to the modulation index, where the power factor of the inverter side is 0.8. All currents are normalized to the inverter load current.

Fig. 10 shows the rms value of dc ripple currents as a function of displacement angle. As expected, the ripple current is maximum at $\pi/2$, and minimum at 0 and π.

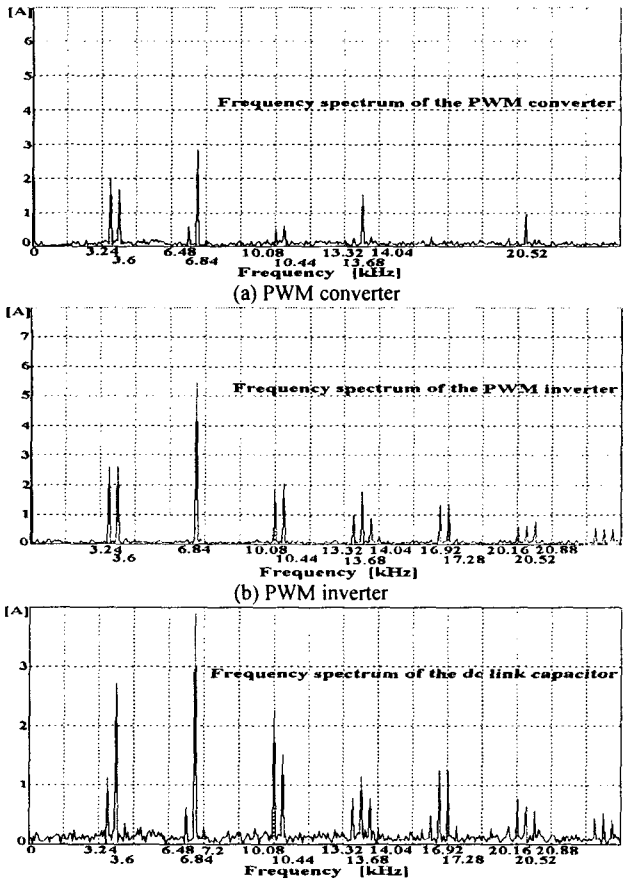

(a) PWM converter

(b) PWM inverter

(c) Dc link capacitor

Fig. 7. Harmonic spectrum of dc link current(simulation)

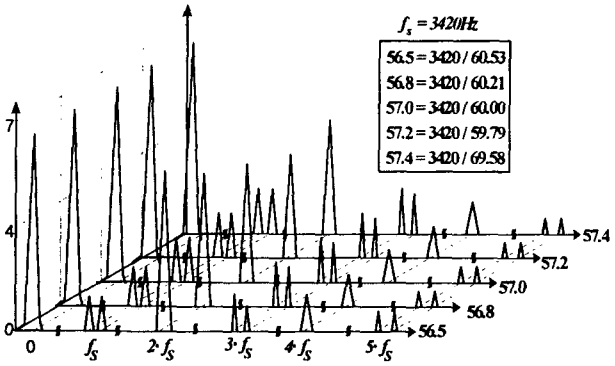

Fig. 8. Harmonic spectrum of inverter input current for asynchronous PWM

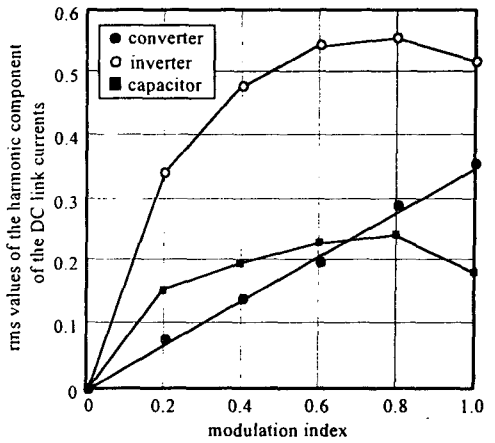

Fig. 9. Dc link ripple currents with regard to modulation index

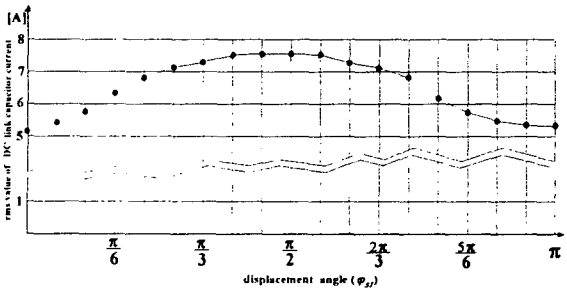

Fig. 10. Rms value of the dc link ripple currents as a function of φ_{st}

VI. CONCLUSIONS

In this paper, an analysis of the dc link ripple currents for the three-phase ac/dc/ac PWM converters has been developed. The analysis is based on the switching function and exponential Fourier series expansion. The analysis results coincide well with those of simulation. The proposed analytic method for the dc link current is useful for selecting the capacitor size, diagnosing the capacitor failure and estimating its lifetime as well as for understanding PWM switching operation.

VII. REFERENCES

[1] Amine Lahyani, Pascal Venet and Guy Grelet, "Design of processing system for state diagonosis of electrolytic capacitors," *EPE Journal*, pp. 19-24, Feb., 2001

[2] P. A. Dahono, Y. Sato, and T. Kataoka, "A novel method for analysis of inverter currents," *IEE Conf.*, pp. 407-412, Oct., 1994.

[3] P. A. Dahono, Y. Sato, and T. Kataoka, "Analysis of ripple components of the input current and voltage of PWM inverters," *INT. J. Electronics*, vol. 80, no. 2, pp. 265-276, 1996.

[4] P. D. Evans and R. J. Hill-Cottingham, "DC link current in PWM inverter," *IEE proc.* on Electric Power Applications, vol. 133, no.4, July, 1986.

[5] L. Sack, "DC link current in bidirectional power converter with coordinated pulse patterns," *EPE proc.*, Trondheim, pp. 239-244(vol. 4), 1997.